Solid Freeform Fabrication 2023: Proceedings of the 34th Annual International Solid Freeform Fabrication Symposium – An Additive Manufacturing Conference
Reviewed Paper

EVALUATING THE COMPRESSIVE STRENGTH OF AM RISERS FOR GREEN SAND METALCASTING

C. R. Hasbrouck[1]* and Samantha A. Melnik[1]

[1]Department of Industrial and Manufacturing Engineering
The Pennsylvania State University, University Park, PA 16802

Abstract

While many metalcasting foundries have experimented with using additive manufacturing (AM) for patternmaking, the compressive strength of the tapered AM risers for green sand metalcasting has not yet been explored. This study investigates the effects of infill pattern type, infill density, and shell thickness on the compressive strength of a standard 3-inch diameter by 5-inch tall by 3-degree taper cylindrical riser manufactured with PLA using a material extrusion process. The findings for these AM risers include plots and mathematical models of compressive strengths at three different scales of the standard geometry (full, three-quarters, and half), predicted build times and masses using other common infill patterns, potential failure mechanisms during use of AM and conventionally manufactured riser patterns, and considerations on design for both additive manufacturing and green sand metalcasting. It is concluded that AM risers can be incorporated into and perform well as part of conventional green sand metalcasting patterns.

Keywords: additive manufacturing, material extrusion, metalcasting, compressive strength, risers, patterns, hybrid manufacturing, desktop printers

Introduction

Metalcasting has spanned centuries of practice and is the backbone of the world's industrial materials industry, with 90% of consumer goods containing cast metal [1]. Through the centuries, metalcasting has seen improvements in efficiency, mechanical properties, cost, part complexity, etc., all the while retaining significant aspects of traditional processes [2]. It has been shown that the appropriate leveraging of additive manufacturing (AM) processes can lead to the improvement of the metalcasting industry, allowing for increased part complexity, reduced lead times, and better prototyping [3].

It is important to have knowledge of traditional metalcasting processes to understand where AM can be beneficial. There are two overarching moldmaking categories of metalcasting: expendable mold and permanent mold processes [4]. Each moldmaking process category has advantages and disadvantages, with the major difference between the two types being the retention of the mold post-casting. In the case of expendable mold processes, the mold is single-use and is either destroyed from functionality or discarded completely post-casting [5]. Likewise, there are two overarching patternmaking categories of metalcasting: expendable pattern and permanent pattern processes [5-8]. Similarly to expendable molds, expendable patterns are considered as single-use while permanent patterns are reused for multiple

*Corresponding author: crh33@psu.edu

castings. However, unlike expendable molds, expendable patterns such as foam and polymer-based materials are completely consumed during the casting process and do not leave any components behind that can be reused for a future expendable pattern [6].

The sand casting process has been in operation since 645 B.C. and remains the cheapest and most widely used metalcasting process, continuing to be a widespread practice in a multitude of manufacturing sectors [2], [9]. Sand casting is an expendable mold metalcasting process that can utilize either permanent or expendable patterns [6], [7]. The expendable sand molds are typically categorized as green sand (silica or a specialty sand bonded with clay and water), or chemically bonded sand which uses a chemical binder [6]. If the mold is made from green or chemically bonded sand, it can be thermally or mechanically reclaimed for re-use as a new expendable mold or discarded entirely if it has lost functionality [6].

In addition to traditionally manufactured sand molds, there are opportunities for additive manufacturing of sand molds via binder jetting processes as explored by Sivarupan et al. [10]. Companies such as ExOne and Voxeljet advertise such capabilities, offering printers with build sizes of 4 m x 2 m x 1 m, layer thicknesses as small as 0.15 mm, and print speeds exceeding 130 L/h [11-12]. Currently, these systems are costly, make use of hazardous binders, and require significant maintenance, thus the integration of such systems within the metalcasting community has been slow. However, Lynch et al. have explored the concept of shared industrial hubs for the use of binder jetting equipment, reducing the burden put upon a single metalcasting company, many of which are small businesses lacking the capital to leverage such technology otherwise [13]. Such industrial hubs for direct production of AM sand molds have not yet been implemented on a widespread basis, but the sand casting community can still currently make use of AM technologies for patternmaking.

It is well known within the sand casting community that patternmaking is a considerable capital investment with substantial lead times for manufacture [14-16]. According to a metalcasting foundry local to the authors, the typical cost of a wooden pattern for a 26-inch by 26-inch by 8-inch flask is approximately $1600, and a similar pattern made from foundry board is about $5000; each has a typical lead time of about two weeks to produce [17]. If a pattern is insufficient in strength, dimensional accuracy, or results in unsound castings, it must be redesigned and remanufactured, further adding to lead times and capital costs. The ability to rapidly prototype or manufacture patterns using additive manufacturing reduces both lead time and capital costs by a considerable margin [15].

As previously mentioned, the expendable mold sand casting process can use either expendable or permanent patterns. Permanent sand casting patterns are often machined from aluminum, wood, or foundry board while expendable patterns are traditionally made of injection molded foam or a polymer [7]. The use of desktop material extrusion processes has led to the in-between category of semi-permanent patterns; these patterns function as permanent patterns but due to their relatively low percentage of solid infill, they tend to either degrade or break more quickly than aluminum or wooden permanent patterns. Such AM patterns are ideal for prototyping new design ideas or for low volume runs of castings [18].

Prior work by Hasbrouck et al. has investigated the dimensional tolerancing capabilities of material extrusion-based patternmaking for green sand casting, including the use of polylactic acid (PLA) for non-critical pattern components and photopolymers for critical pattern components, but did not explore the strength of the patterns [19]. Anakhu et al. studied the effects of infill density, print layer height, and number of solid layers for optimum PLA plastic compressive strength [20], which is an important metric for determining the ability of the pattern to survive the compaction forces of sand required for moldmaking in green sand casting processes. Pernet et al. studied additively manufactured PLA's compressive strength while varying the infill styles and percentages within the ASTM Standard D695-15 [21] test geometry, concluding that 2D infill patterns perform the most favorably when comparing load-to-weight ratios because of the alignment of the mechanical supports to the direction of the load. Harshit et al. performed a similar study of the compressive strength of additively manufactured PLA using ASTM Standard D695-15 [22], investigating the effects of layer height, infill density, and print speed on part strength and demonstrating optimal strength at a layer height of 0.2 mm, infill density of 80%, and print speed of 40 mm/min. There are many other studies [23-33] which analyzed the effects on various mechanical properties of material extrusion-produced materials such as acrylonitrile butadiene styrene (ABS), polycaprolactone (PCL), polycarbonate (PC), PLA, PLA with an acrylic modifier, and ULTEM 9085 when modifying AM variables such as infill density, infill width, build orientation, laydown pattern, layer thickness, color, nozzle temperature, shell perimeters, and infill patterns.

This case study focuses on the advancement of desktop material extrusion AM processes for nonferrous sand casting operations for the production of semi-permanent reusable patterns in the patternmaking process. There is a national interest in reshoring and revamping manufacturing capabilities in the United States by investing in development and integration of cutting edge technologies, as evidenced by state initiatives such as the Manufacturing PA Initiative in Pennsylvania [34]. In this vein, a nonferrous green sand metalcasting foundry, Erie Bronze and Aluminum Company ("Erie Bronze"), has experimented with AM for patternmaking in the past but gave up after the parts did not reduce lead time or meet strength requirements. The company expressed continued interest in the idea but needed assistance in determining printing parameters that resulted in a reduction in lead time while still meeting the minimum strength requirements for the forces imparted to the patterns by their molding practices. Erie Bronze uses both automated (Figure 1, (a)) and manual (Figure 1, (b)) green sand molding lines, each of which result in different force magnitudes and distributions across the patterns.

Erie Bronze is a relatively small foundry that mainly functions as a "job shop" with typical run quantities of as low as one and as high as 1000 parts [17], making it an ideal candidate for AM semi-permanent patterns. The automatic molding line outputs a pressure reading of 700 psi [35], but it is unclear whether that is the hydraulic cylinder pressure, the pressure the flask sees overall, or the pressure the pattern parts see. Therefore, instead of trying to optimize the patterns for their ideal strength for this single application, the research presented in this study focuses on compressive strengths obtainable across a wide range of infill densities.

Figure 1: Molding lines at Erie Bronze and Aluminum Company: (a) automatic, and (b) manual. Published with permission.

All green sand metalcasting patterns must contain a sacrificial rigging system to supply liquid metal to the part to be cast [5], [8]. Most metalcasting rigging systems contain at least one sacrificial volume of metal called a riser to feed the shrinkage that happens as the metal experiences a phase change during solidification from liquid to solid [36]. These risers are designed to meet solidification rules dependent on such variables as alloy shrinkage percentages, the volume of the casting to feed, feeding distance, thermal properties of the mold, and more [37] and are optimized to solidify after the rest of the casting system components. Therefore, the larger the volume-to-surface area ratio is according to Chvorinov's rule [38], the better the riser due to the maximization of volume of metal coupled with the minimization of lowest cooling rates from conduction across the mold surfaces. Based on Chivornov's rule, the ideal riser shape is a sphere. However, since spheres are difficult to mold for green sand patterns, tapered cylinders are most typically used instead. As these volumes of metal are sacrificial, their dimensional tolerances are less stringent than the functional surfaces of the actual cast part(s). Combining this knowledge with the relatively standardized riser geometry and frequency of its use across sand casting patterns led the authors to focus on risers for this case study. A nominal riser size of 3-inch diameter by 5-inch height by 3° taper as provided by Erie Bronze was used as a basis [17], [19]. An example of a matchplate featuring an AM semi-permanent pattern cope (a) and drag (b) used for green sand casting is shown in Figure 2, where the parts of interest are identified by blue ovals and the risers are indicated by orange arrows [19].

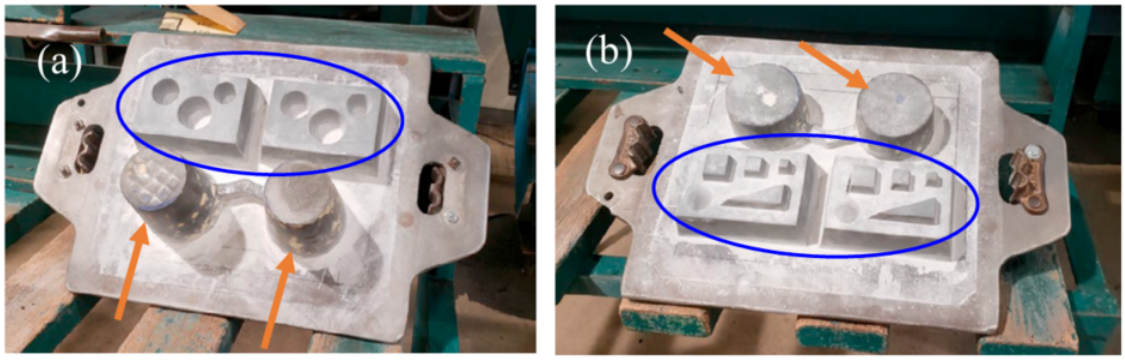

Figure 2: Matchplate (a) cope – top half, and (b) drag – bottom half, for green sand castings featuring additively manufactured patterns [19].

The work for this study was completed with input from Erie Bronze to best solve their particular production issues. The results of this study can be reasonably extended to other nonferrous, small-quantity "job shop" type metalcasting foundries utilizing low-pressure molding techniques with desktop material extrusion-produced patterns. More research is necessary for metalcasting patternmaking practices that require higher temperatures, higher molding pressures, or more use cycles. The remainder of the paper documents the research questions explored, the experimental methodology used, and the results of the study.

Research Questions

Five research questions (RQ) and associated hypotheses (H) were developed to help metalcasting patternmakers design for additive manufacturing of risers:

RQ1: Does infill density (percentage) affect the print time, mass, compressive strength, dimensional stability, or surface roughness of additively manufactured risers of a standard length-to-diameter ratio?

H1: The infill density (percentage) will have a significant effect on print time, mass, and compressive strength but not on dimensional stability or surface roughness.

RQ2: Does shell thickness affect the print time, mass, compressive strength, dimensional stability, or surface roughness of additively manufactured risers of a standard length-to-diameter ratio?

H2: The shell thickness will have a significant effect on compressive strength and surface roughness but not on print time, mass, or dimensional stability.

RQ3: Does infill type (pattern) affect the print time, mass, compressive strength, dimensional stability, or surface roughness of additively manufactured risers of a standard length-to-diameter ratio?

H3: The infill type (pattern) will have a significant effect on print time, mass, and

compressive strength but not on dimensional stability or surface roughness.

RQ4: Does filament color affect the print time, mass, compressive strength, dimensional stability, or surface roughness of additively manufactured risers of a standard length-to-diameter ratio?

H4: Filament color will have a significant effect on compressive strength but not on print time, mass, dimensional stability, or surface roughness.

RQ5: What are the print time, mass, compressive strength, and dimensional stability capabilities at various infill densities of additively manufactured risers of a standard length-to-diameter ratio for a constant infill type, shell thickness, layer height, and filament color?

H5: The print time, mass, and compressive strength will all increase with increased infill densities across all scales. Dimensional stability will decrease as scale decreases but will not be affected significantly by infill density.

Experimental Methodology

This initial case study explores the use of material extrusion of polylactic acid (PLA) filament. Material extrusion was chosen due to its widespread availability, compact (desktop) nature, and relatively low capital, operating, and maintenance costs. PLA was chosen also for its widespread availability and low cost as well as its ease of printing and relatively good mechanical properties. Test specimens of a representative riser geometry were produced using two Prusa MK3S series printers. Infill pattern, density, and shell thickness were varied to test which combination provided optimal printing parameters. Limiting cost and lead time are the two most important considerations for AM patterns for metalcasting, provided that the parts produced can withstand the forces of moldmaking and hold up dimensional tolerances to sand abrasion and moisture absorption over time. Thus, initial narrowing of parameters was done with that consideration in mind as to ensure significant lead time or cost was not incurred during the printing process, which would negate the benefit of its implementation. Upon narrowing down the printing parameters, parts were printed in three size scales to investigate the effects of part size on results. Following printing, parts were compression tested to identify the yield strength of the various test specimens, to determine if AM risers were suitable for green sand operations.

Materials

Due to supply chain issues at the time of ordering filament, only a glitter filament was available to be procured in a quantity large enough for this study. A total of 15 kg of opal green Prusament PLA were ordered for this case study. It is important to note that the presence of glitter may affect both the mechanical and optical properties of the final parts depending on what is causing the glitter effect. For example, the presence of metallic powder [39] may cause the glitter effect, which can result in greater strength and further increases in brittleness [40] as well as increased nozzle wear [41]. While these parameters

were not explicitly explored for this case study, it will be discussed how the presence of glitter negatively affected the ability to perform optical profilometry measurements on the printed parts.

Fabrication and Physical Measurements

To begin, a nominal riser size of 3-inch diameter by 5-inch height by 3° taper as provided by Erie Bronze [17] was modeled in SolidWorks. It was exported to a STL file using American Standard Code for Information Interchange (ASCII) encoding, inch reference dimensions, and custom tolerance settings of 0.00032527-inch deviation tolerance and 0.5 degree angle tolerance. These settings provided the highest available quality STL file export from SolidWorks to minimize geometry losses to triangulation. Two different slicer softwares were used for this case study: Ultimaker Cura and PrusaSlicer. PrusaSlicer, unlike Ultimaker Cura, allowed for greater customization of part g-code when combined with the Prusa-branded printers; however, Ultimaker Cura was also employed, as it is one of the most commonly used open-source slicer softwares in the 3D printing community. Comparisons regarding print time and material requirements were made between the two softwares to ensure that the results were independent of the slicer software used. Two different pre-assembled Prusa material extrusion desktop printers were used: an Original Prusa i3 MK3S with orange trim, and an Original Prusa i3 MK3S+ with black trim.

The printers were referred to by trim color instead of model number throughout data collection. The height and bottom diameter of each printed part were measured using 8-inch Mitutoyo Digimatic digital calipers (Figure 3) with an accuracy of ± 0.0005 in (model number CD-8"ASX). For measurements of mass, a WeighMax digital postal scale with an accuracy of ± 3g (model number W-BC130) was used. To avoid user bias in the measurements, the same person performed all mass and dimensional measurements.

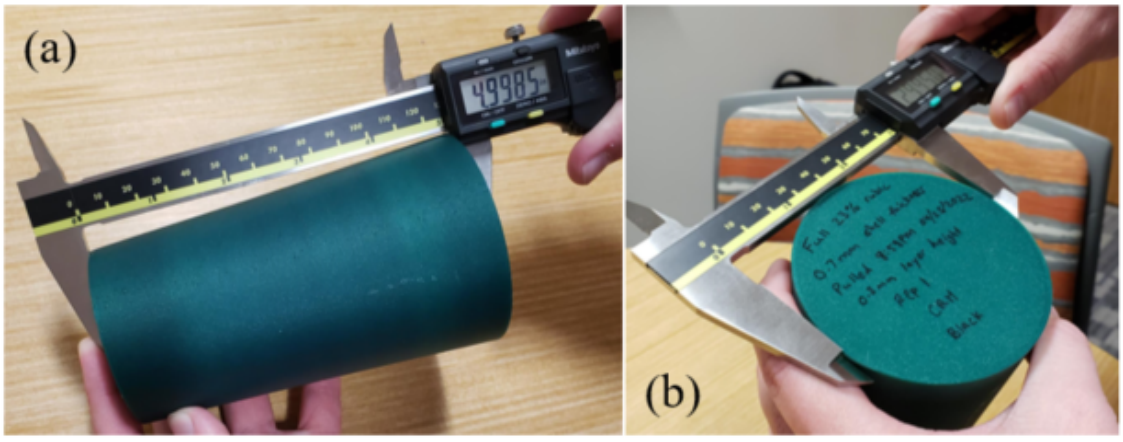

Figure 3: Measuring an AM riser with digital calipers: (a) height, and (b) diameter.

Documentation

A print log was kept throughout the study that included the following information for every print: DOE number and quadrant or scale, shell thickness, infill pattern, infill density, print start time and date, print stop time and date, print pull time and date, initials of who pulled the print, the printer used, the filament roll ID number, the filament roll tolerance, and the filament roll manufacturing date. An additional log for the measurements of each print was kept with the following information: DOE number and quadrant or scale, replication number, infill density, mass (g), print time (hr), height (in), diameter (in), initials of who measured the part, and the date the part was measured. Finally, on the bottom of the printed parts, identification of DOE number and quadrant or scale, shell thickness, infill pattern, infill density, print pull time and date, initials of who pulled the print, and the printer used were marked. Three replicates of each build parameter condition were printed on a single build plate.

Surface Roughness

Any surface roughness measurements on AM parts were performed using a Zygo Zegage optical profilometer shown in Figure 4.

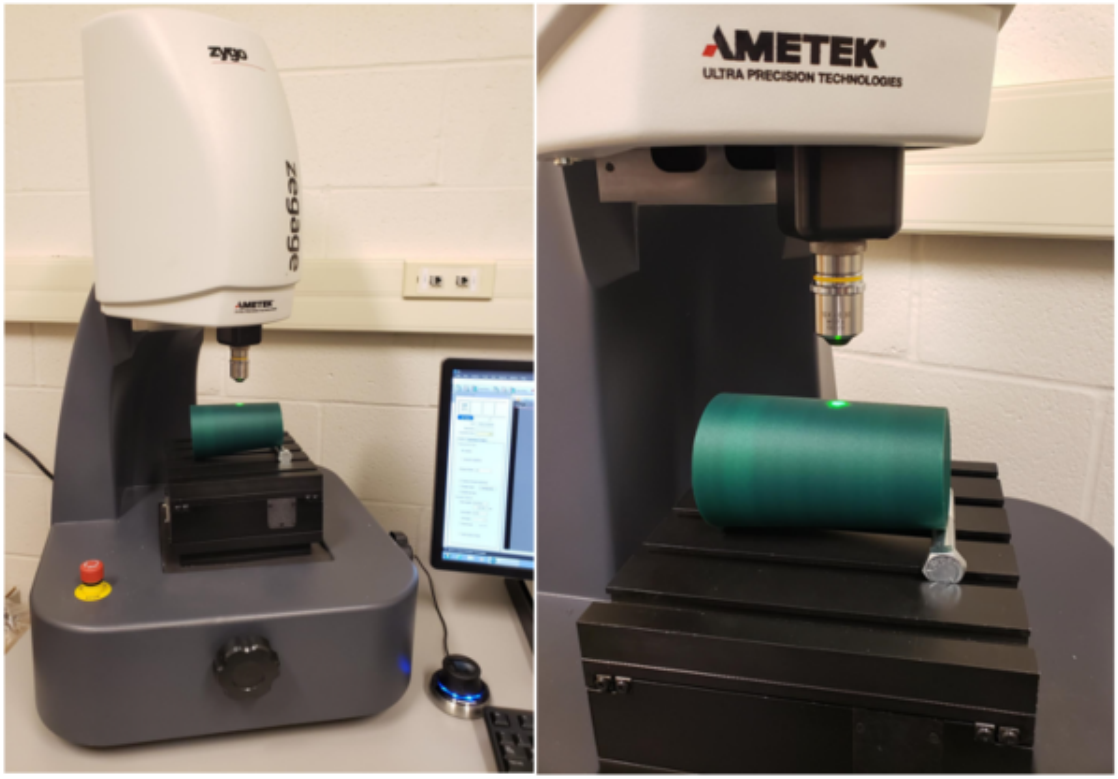

Figure 4: Optical profilometry setup for AM risers.

A 10X Mirau lens was calibrated with either 200 or 500 µm pitch square patterns on a standard Zygo calibration block . A scan area/field of view of 830 µm by 830 µm was used

with a scan depth of 1200 µm, resulting in a scan time of about 155 seconds for each part. Data was analyzed using Zygo Mx software employing conical form correction and $\pm 3\sigma$ spike clip surface processing filters.

Compression Testing

Compression testing was carried out using a Tinius Olsen 120-kip universal testing machine (model number 120K Super L). Data was collected and initially plotted with the Tinius Olsen Test Navigator software. The machine was programmed to run a compression test from position data in four sequential steps:

1. Move at a position rate of 0.5 in/min until a force value of 50 lb_f is reached
2. Zero channel force
3. Zero channel position
4. Move at a position rate of 0.1 in/min until a position of 1 inch is reached

Step 1 ensures the load cell is operating correctly and the part is touching both platens. Steps 2 and 3 clear the current force and position readings back to zero to perform the compression test. Step 4 is the compression test and was modified for each scale to stop at a position equal to 20% of the height of the sample or until a sample break was detected (75% or larger drop off in peak load), whichever came first. The data was automatically exported as a graphical image and as a comma-separated values (csv) file for both load (lb_f) and stress (psi) versus position (in). The software automatically reported yield strength based on the 0.2% offset rule. Yield strength was chosen as the indicative strength over ultimate strength for two main reasons: (1) once the part has yielded to plastic deformation, the dimensions are no longer suitable for a metalcasting pattern, and (2) many parts never peaked or fractured at what could be considered an ultimate strength. Before each test, the sample name was inputted along with its height and the bottom (larger) diameter of the part.

The compression testing setup is shown in Figure 5. Two test setups were run before the real testing to ensure the program ran as intended. First, two aluminum cans were crushed using the program to test the initial force readout and consequential zeroing of the channels as well as return of the crosshead upon reaching a position of one inch. Next, four dummy parts were printed using galaxy silver Prusa PLA, two at 15% cubic infill and two at 50% cubic infill. The dummy plastic parts were run to examine the sensitivity of the load cell, determine approximate low and high ends of strength of the parts, and determine possible failure mechanisms.

Designs of Experiment

To determine the best parameters to proceed with for the full experimental study, three designs of experiment (DOEs) were completed. All three DOEs used a two-level full factorial design with three replications and focused on the full-scale riser size with nominal dimensions. To reduce print time as much as possible, a large layer thickness of 0.3 mm was used and

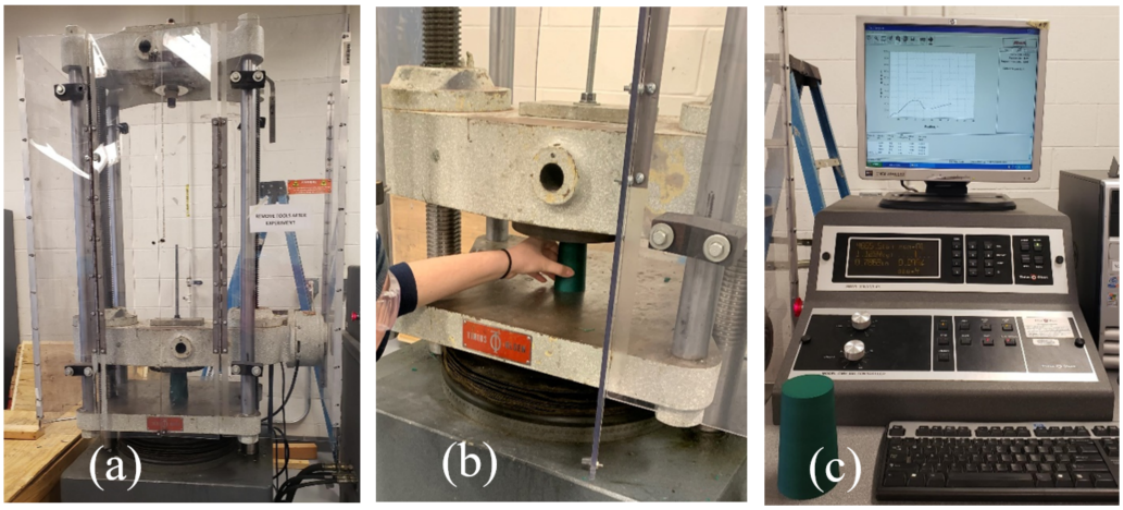

Figure 5: Tinius Olsen 120-kip universal testing machine compression testing setup: (a) full view of machine, (b) loading a sample into the machine, and (c) data collection screen.

held constant for all prints. The first DOE aimed to answer RQ1 and RQ2 and investigated the significance of shell thickness and infill percentage on print time, mass, compressive strength, dimensional stability, and surface roughness. A gyroid infill was chosen and held constant, the high and low values for shell thickness were 1.4 and 0.5 mm, respectively and the high and low values for infill density were 50% and 15%, respectively. Similarly, the second DOE focused on RQ3 and investigated the significance of infill pattern on print time, mass, compressive strength, dimensional stability, and surface roughness. A nominal shell thickness of 0.7 mm was chosen and held constant, the high and low values for infill pattern were gyroid and cubic, respectively (Figure 6) and the high and low values for infill density were 50% and 20%, respectively.

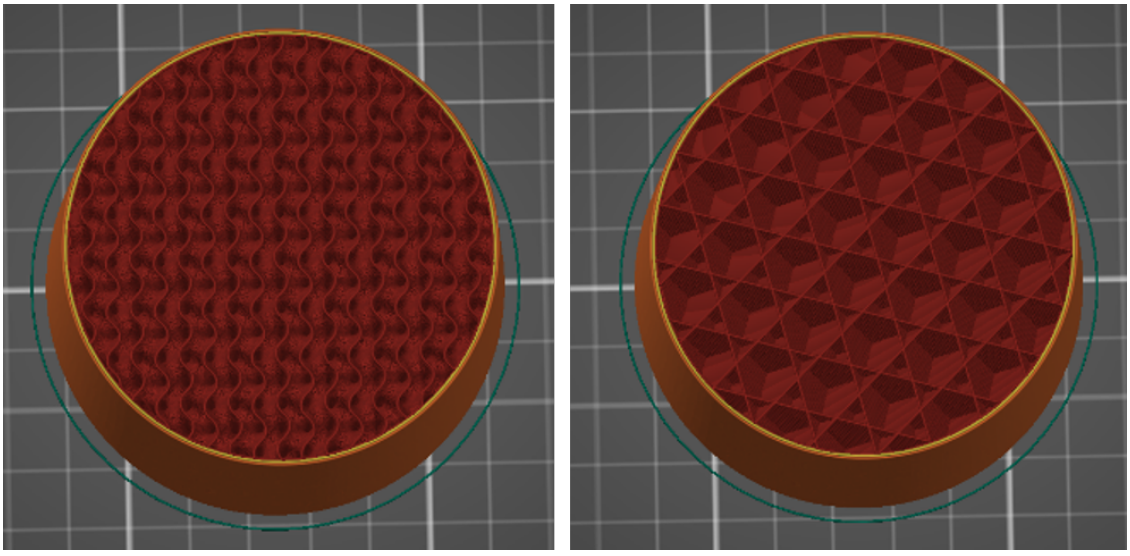

Figure 6: DOE infill patterns - (a) gyroid infill, and (b) cubic infill.

Finally, the third DOE focused on RQ4 and investigated the significance of filament color on print time, mass, compressive strength, dimensional stability, and surface roughness. A nominal shell thickness of 0.7 mm and infill pattern of cubic were chosen and held constant, the high and low values for filament color were pineapple yellow and opal green, respectively and the high and low values for infill density were 50% and 20%, respectively. Ultimaker Cura was used as the slicer for the DOEs because it provides additional manual settings for customization of shell thickness parameters over PrusaSlicer. All DOE data collected were analyzed using standard analyses of variance (ANOVAs).

Full Experiments and Compression Tests

Upon completion of the three preliminary DOEs, a full experimental design was developed to answer RQ5. The nominal riser dimensions were used and explored at three scales: full-scale, three-quarter scale, and half-scale. The layer thickness of 0.3 mm was continued to be held constant, as were the nominal shell thickness of 0.7 mm and filament color and brand of Prusament opal green PLA. A standard cubic infill pattern was chosen for the full experimental study due to its relatively high strength-to-weight ratio and significantly decreased print time over gyroid. Each scale of the nominal length-to-diameter ratio risers was completed with infill densities varying from 5-50% in increments of 5%. Each infill density had three replicates, all built on a single build plate. It is important to note that printing three replicates on a single build plate resulted in increased time between printing of layers than would normally be seen if printing one part at a time and could contribute to a slight decrease in mechanical properties. All full experimental data collected were analyzed using standard analyses of variance (ANOVAs) and linear regression modeling, where applicable.

An attempt was made to replicate as closely as possible what metalcasting foundries would do if performing these experiments in-house. Therefore, time between print completion and compression testing was left relatively randomized and all replicates were built on a single build plate whenever possible. Additionally, advanced design for additive manufacturing (DfAM) concepts such as topological optimization, customized infill lattices, and graded infill patterns were not explored.

Wooden Risers

As discussed in the *Experimental Methodology* section, Erie Bronze typically uses wooden patterns for their automatic green sand molding machine. Since the 700 psi pressure reading provided by the company is not conclusive enough for designing an optimized plastic riser with infill pattern and density to reach the necessary strength, a generalized approach to determine achievable strengths with different DfAM parameters was employed instead. Erie Bronze graciously supplied the authors with sets of pine wooden risers from patterns up to 20+ years old as well as new wooden risers ordered special from the pattern shop for this case study. The risers from the old patterns were at least partially coated for smoothness and contained additional pieces from gating system that were removed before testing. The wooden risers that were manufactured for this project were made to be the same scale as

those plastic parts printed and tested. Examples at each scale of the old wooden risers, the newly manufactured wooden risers, and the plastic risers are shown in Figure 7.

Figure 7: Old wooden risers and new wooden risers next to their printed plastic counterparts at each of the three scales.

Both the old and new risers consisted of between two to four pieces of wood assembled together, and the layer/grain orientation could be either vertical or horizontal. Examples of the different wood layer orientations are shown in Figure 8. Wood is an orthotropic material, so the properties depend greatly on the orientation of the grains [42]. Additionally, the strength and dimensional stability of wood is highly dependent on knot content and location and the moisture content [42].

Figure 8: Examples of wooden layer assembly orientations: horizontal (left) and vertical (right).

Results and Discussion

Four distinct datasets were produced during the data collection phase: three DOE datasets and one regression dataset. Data collected for each of the three DOEs included: mass (g), height (in), diameter (in), surface roughness (Sa, Sz, Sq), print time (hr), compressive yield strength (lb_f and psi), break percentage (%), and the elastic modulus (Mpsi). Analyses of variance (ANOVAs) at an alpha significance level of 0.05 were run for each parameter, considering the factors for the corresponding DOE.

DOE 1 – Infill Percent and Shell Thickness

The significance of infill percent (low level: 15%, high level: 50%) and shell thickness (low level: 0.5 mm, high level: 1.4 mm) were studied in DOE 1. Results indicated neither shell thickness, infill percent, nor their interaction significantly affected riser height, diameter, or surface roughness. Surface roughness results were difficult to acquire optically due to glitter within the filament. Mechanical measurement techniques were attempted using a Mahr Pocket Surf IV surface roughness gauge; however, the roughness of the parts was beyond that of the equipment's maximum measuring capabilities of 250 µin Ra. Therefore, while such factors were not deemed significant for the surface roughness, additional work in this area is needed to verify the results.

Infill percent, shell thickness, and their interaction significantly affected the parts' compressive yield strength (lb_f and psi), as well as the elastic modulus. Shell thickness was the only significant factor for break percentage. While shell thickness was found to

significantly affect compressive yield strength (positively favoring 1.4 mm over 0.5 mm), visual inspection overrode the results. Both the high and low shell thickness values resulted in a vertical seam along the height of the cylindrical risers, pictured in Figure 9.

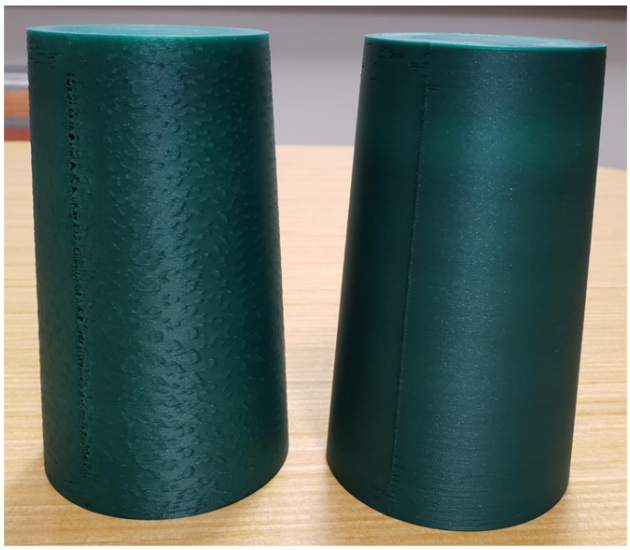

Figure 9: Vertical seams along PLA risers. 0.5 mm shell thickness (left); 1.4 mm shell thickness (right).

While the risers are sacrificial parts, the seams alongside the risers would require additional post-processing to ensure a smooth finish or risk sand entrapment, adding extra time and cost. Printed risers at a nominal shell thickness of 0.7 mm (standard for 0.3 mm layer height in Prusa Slicer) did not produce a vertical seam. Thus, the authors moved forward with the nominal shell thickness for future experiments.

DOE 2 – Infill Percent and Infill Type

The second DOE studied the effects of infill percent (low level: 20%, high level: 50%) and infill type (low level: cubic, high level: gyroid). Initially, DOE 2 was designed as a two-factor three-level full-factorial, with infill percent values of 20%, 50% and 80% and infill types gyroid, cubic, and honeycomb to replicate the case study published by Dev and Srivastava [43]. During the slicing process the experiment was redesigned, as infill percentages above 50% across all infill types began to eliminate the lead time advantages of AM over traditional patternmaking. The same reasoning led to the removal of the honeycomb infill pattern, which had a significantly longer print time across all infill percentages as compared to the cubic and gyroid infill patterns. Gyroid and cubic infill patterns were chosen as they are standard infill types found on most of the commercially available and open-source slicing software and have a favorable strength-to-weight ratio.

Results from DOE 2 indicate infill type significantly affected riser diameter, whereas the interaction between infill type and infill percent significantly affected surface roughness. Though, similar to that of DOE 1, additional work is needed to verify the surface roughness

results. Additionally, infill percent significantly affected the parts' elastic moduli. Infill percent, infill type, and their interaction significantly affected riser height, mass, and compressive yield strength (lb_f and psi). At 20% infill, risers with gyroid infill were 0.57% stronger than parts with cubic infill. However, at 50% infill, parts with cubic infill were 2.6% stronger than those with gyroid infill. Given the substantially lower print times and mass requirements for the cubic infill, as well as the minimal difference in strength at the 50% infill mark, the authors chose to use cubic infill for the remaining experiments.

DOE 3 – Infill Percent and Filament Color

The third DOE focused on color type (low level: opal green, high level: pineapple yellow). Due to supply chain issues and filament availability at the time of the study, the risers were initially printed in Prusament opal green PLA filament, which contains glitter. As discussed in the *Experimental Methodology* section, it is known that presence of glitter elements can affect mechanical properties of PLA. It has also been proven that the color of PLA filament can affect tensile strength of PLA parts [44]. To test the significance of PLA color on compressive strength, and in an attempt to acquire optical surface finish data, parts at 20% and 50% cubic infill were reprinted in Prusament pineapple yellow PLA to evaluate potential significance. Both infill percent, infill type, as well as their interaction were deemed significant factors affecting the parts' compressive strength (lb_f and psi), with yellow found to be favorable. Surface roughness characteristics were also analyzed, but the bright color of the pineapple yellow filament proved to be just as difficult to measure optically as the glitter within the opal green filament, and the results were found to be insignificant.

Full Experiment – Mathematical Models

Using the results from the first three DOEs, the optimal riser design to increase compressive strength was 50% cubic infill with a shell thickness of 1.4 mm printed in pineapple yellow Prusament PLA. Due to the issues with filament availability and post-processing, the optimum riser design was instead 50% cubic infill with a shell thickness of 0.7 mm printed in opal green Prusament PLA. However, as infill percent increased, so too did the mass and print time of the part, resulting in increased costs and lead time which foundries are hoping to reduce. Thus, infill percent was varied from 5% to 50% cubic infill in 5% increments to provide designers with a mathematical relationship between compressive strength and cubic infill percent, allowing them to pick the appropriate infill percent for their strength needs. Parts were also varied in scale (full-scale, three-quarter scale, and half-scale) while maintaining their length-to-diameter ratio. This was done to verify the model for the specified length-to-diameter ratio, as well as to test the potential differences between the scales. All calculations for regression models and linear coefficients of determination (R^2) were done using MATLAB.

Initially, the *polyfit* command was used to produce third-order regression models. Across all scales, the third-order models did not produce as close of a fit as hoped due to the presence of outliers. The models were re-run for a first order (linear) regression by removing a single outlier from the full-scale and half-scale data, resulting in a closer fit. The linear regression

equations and corresponding R^2 values are listed in Table 1.

Table 1: Linear fit equations and R^2 values.

Scale	Equation	R^2
Full	y = 276.812*x - 469.733	0.982
3/4	y = 174.076*x - 162.200	0.982
Half	y = 90.410*x - 160.667	0.88

An example of the compression strength linear regression data for the full-scale risers with the associated equation is shown in Figure 10.

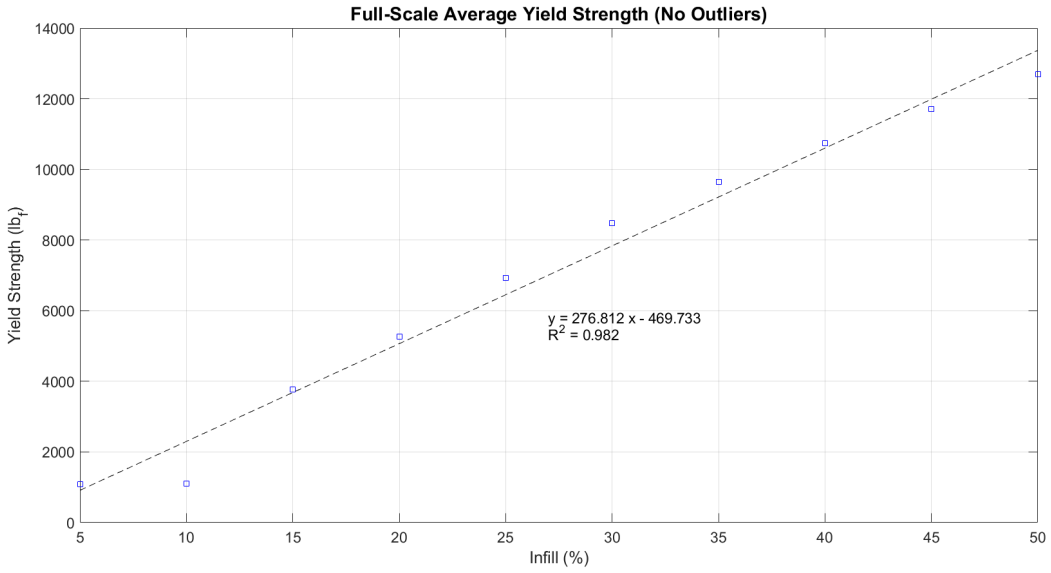

Figure 10: Full-scale, linear regression for compressive yield strength with outliers removed.

Upon re-inspection of the data, the authors found that what were previously thought to be outliers were incorrectly reported measurements, an issue which arose due to the Tinius-Olsen universal testing machine data collection software. As illustrated by the machine-supplied load versus position plot in Figure 11, some graphs exhibited two distinct linear regions.

In certain cases, the software which calculated the 0.2% offset had difficulties determining the appropriate linear region, providing the higher yield point values by mistake. Thus, the compressive strength values resulting from the infill percentages below 20% (at the full- and three-quarter scales) should be ignored for this study.

Print Time and Mass Estimations

Given the material and time constraints associated with this initial case study, alternative infill types were not printed for experimental testing. Instead, print times and masses were

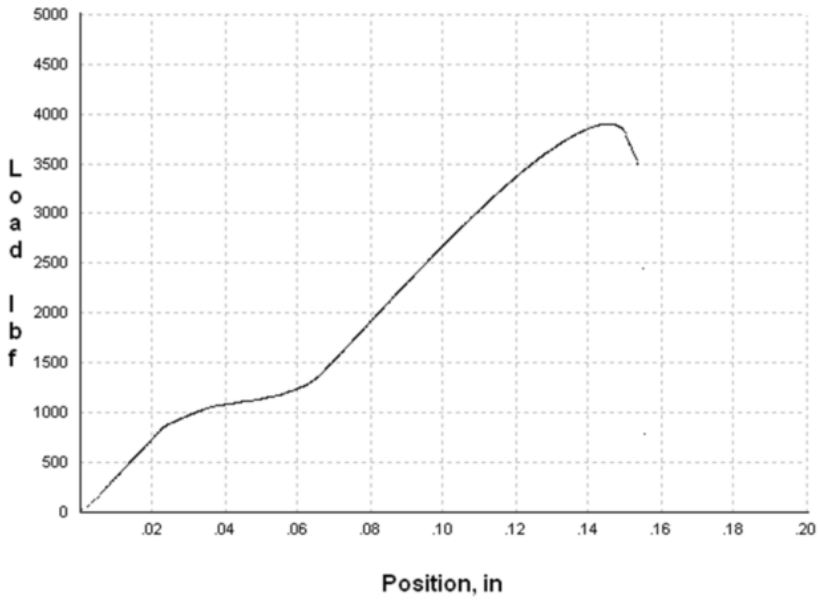

Figure 11: Load vs. Position graph supplied by Tinius-Olsen software highlighting the two linear regions.

estimated using the PrusaSlicer software for six different infill patterns (3D patterns: gyroid, cubic, 3D honeycomb; 2D patterns: honeycomb, concentric, and grid) ranging from 5% to 100% in 5% increments. The infill pattern cross sections can be seen in Figure 12.

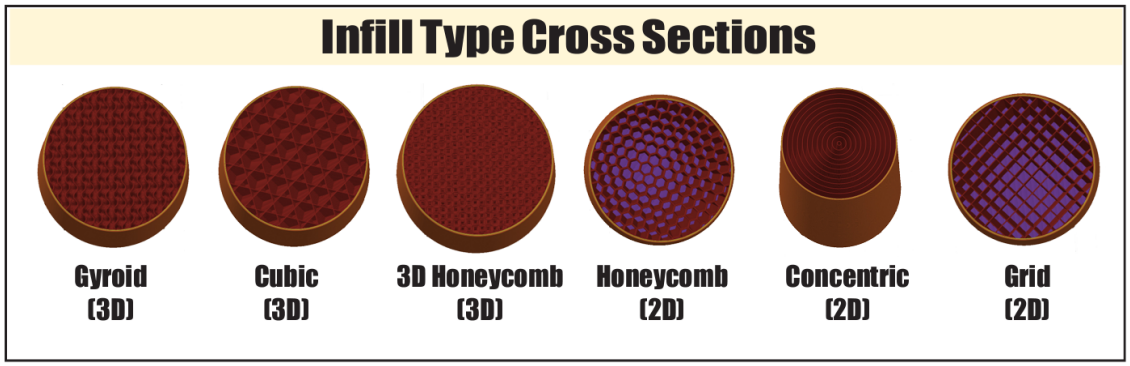

Figure 12: Infill pattern cross-sections.

An example of the plots produced to estimate print time and mass based on scale and infill pattern is shown in Figure 13 for the full-scale risers.

Surface Finish Results

Surface finish data was collected for wooden risers (uncoated and coated) as well as plastic (Prusament PLA) risers. Two methods of collection were used: optical and mechanical.

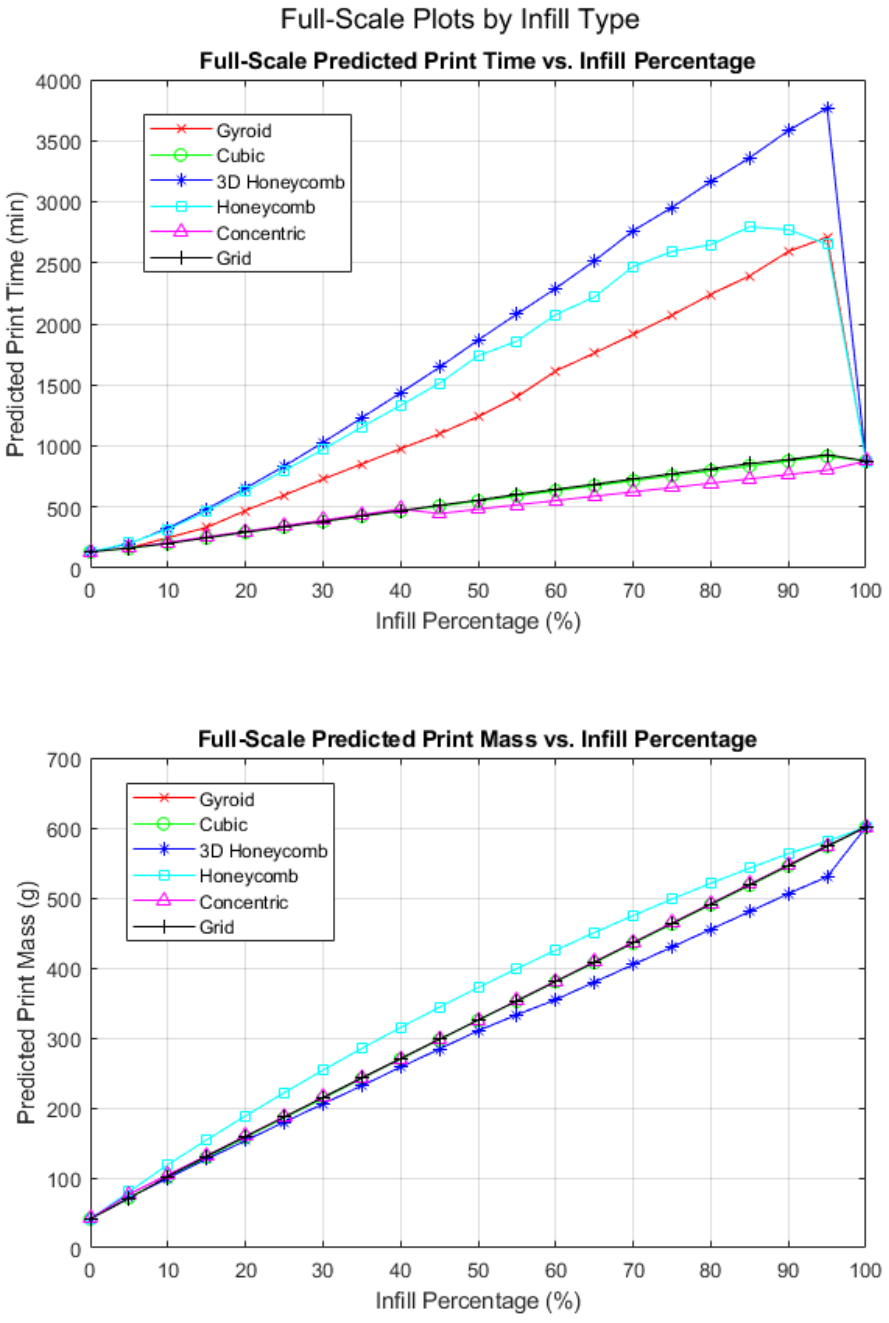

Figure 13: Full-scale print time and mass estimations by infill pattern type.

Optical methods provided average surface area roughness (Sa) values, whereas mechanical methods provided average linear roughness (Ra) values, due to differences in the measuring techniques. While the resulting outputs are not exactly the same, Sa is an extension of Ra

and so the values can be compared to one another for rough analysis.

Table 2 provides the corresponding values for the wooden and plastic risers. Uncoated and coated wooden risers were provided by Erie Bronze. All wooden riser measurements were completed using mechanical methods. The minimum roughness value of the uncoated wooden risers was 81 µin. Comparatively, the coated wooden risers had a minimum roughness value of 29 µin, a 52 µin difference. It is important to note that the coated risers were utilized for upwards of 20+ years in a green sand foundry, leading to abrasive wear and storage degradation of the coating. Thus, newer coated risers are expected to have lower minimum roughness values. Both the coated and uncoated wooden risers had maximum roughness values above 250 µin, the maximum range of the Mahr Pocket Surf roughness gauge for Ra measurements.

Table 2: Surface finish results (μin).

Uncoated Wood - Mechanical	Min Max	81 >250
Coated Wood - Mechanical	Min Max	29 >250
Plastic - Optical	Min Max	207 343
Plastic - Mechanical	Min/Max	>250

Regarding the plastic risers, measurements were attempted both mechanically and optically. Similarly to portions of the uncoated wooden risers, the roughness of the plastic parts surpassed that of the mechanical equipment's maximum measurement capabilities of 250 μin; thus it was concluded that the surface roughness of all the plastics parts was above 250 μin. Optically, a minimum surface roughness of 207 μin was found, whereas the maximum was 343 μin. An example of an optical profile (with units of μm) can be seen in Figure 14.

Note that the output of the figure is in μm; the data was converted to μin for direct comparison to the results gathered mechanically from the wooden parts. Additional work is needed here to further evaluate the surface roughness of the plastic risers, as there were issues obtaining the surface roughness data optically due to the presence of deep layer lines and glitter present in the filament.

However, from the data collected, it can be generally concluded that the uncoated and coated wooden risers are less rough than the plastic risers. Therefore, post-processing in the form of smoothing or coating the plastic risers will likely be needed for metalcasting moldmaking process implementation purposes.

Wood Analysis

The mean and standard deviation of the compressive yield strength (lb_f and psi) were calculated across the three testing scales (full-scale, three-quarter scale, and half-scale). The

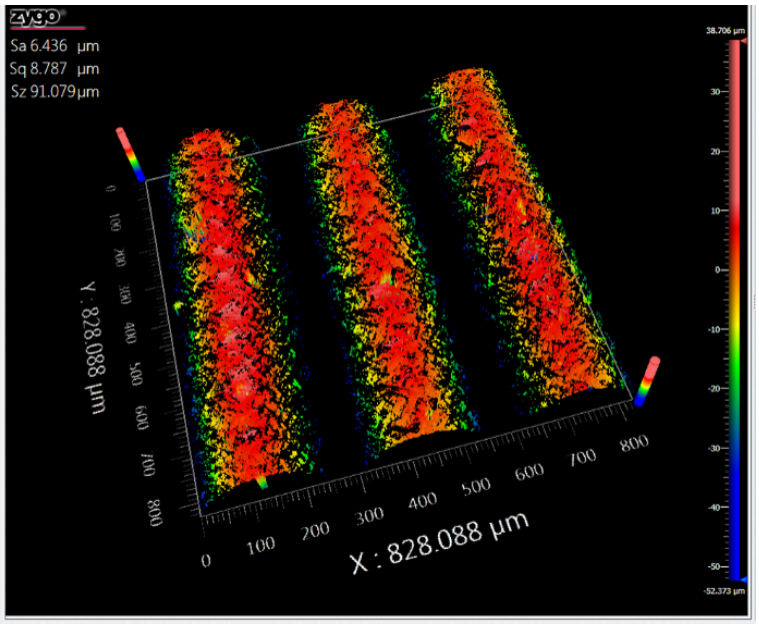

Figure 14: Example optical profilometry output.

average yield strength of the full-scale, uncoated wooden risers (Table 3) was found to be 12,426.67 lb_f, which is approximately equivalent to Prusament PLA risers with a cubic infill of about 45%. However, the standard deviations for both the full and three-quarter scales are equal to approximately 100% of the compressive yield strength mean, indicating a high level of variability across the results.

The authors believe such variability may be related to grain orientation, moisture content, or knot location among other wood property considerations. Some wooden risers were also comprised of multiple parts glued together leading to a visual seam (either horizontal or vertical). Thus, seam orientation is another factor to consider since wood is highly orthotropic in properties due to grain structures. It is also possible that in some cases the strength of the glue is being tested rather than the wood itself.

Table 3: Wood compressive yield strength data.

Scale	Avg. YS (lb_f)	Std. Dev. (lb_f)	Avg. YS (psi)	Std. Dev. (psi)
Full	12426.6667	13487.0358	1757.3333	1907.5865
3/4	8230.0000	8169.4492	2069.0000	2054.0694
Half	563.5000	24.7487	319.0000	14.1421

Dimensional Tolerances

Minitab was used to evaluate the dimensional accuracy of the wooden parts for both height and diameter. Hypothesis testing was run at an alpha significance level of 0.05. The expected mean correlated to the modeled height and diameter of the nominal riser at each

scale.

For the wooden risers, only the height at three-quarter scale was found to reject the null hypothesis, indicating that it was not statistically equivalent to the expected mean. All other scales for both diameter and height were statistically equivalent to their corresponding scale's dimensions. The results for the wooden risers can be found in Table 4.

Table 4: Wood dimensional tolerances for height (in). Note: Using the 95% confidence intervals, LB = Lower Bound, UB = upper bound.

Scale	Mean	Std. Dev.	LB	UB	Tolerance	p-value
Full	5.006	0.0056	4.992	5.02	0.028	0.206
3/4	3.7785	0.0091	3.7559	3.8011	0	0.032
Half	2.512	0.0099	2.4231	2.6009	0.1778	0.336

Plastic dimensional tolerances can be found in Table 5. As can be seen by the low p-values, height and diameter are not statistically equivalent to the expected scales' mean for both full-scale and three-quarter scale plastic risers. At the half-scale, the height was found to be statistically equivalent however the diameter was not. While the plastic risers' expected means do not fall within the measured lower and upper bounds, their dimensional tolerances (or spread) are much lower than that of the wooden risers. The plastic risers generally displayed a tolerance of a couple thousandths of an inch, whereas the wooden risers showed tolerances between a couple hundredths to a couple tenths of an inch. Thus, the difference of actual dimensions to desired dimensions of the plastic risers can be accounted for ahead of time in order to meet the expected values. This should pose no difficulties to foundry designers who are already used to accounting form patternmaker's shrink when designing foundry patterns.

Table 5: Plastic risers dimensional tolerances for height (in). Note: Using the 95% confidence intervals, LB = Lower Bound, UB = upper bound.

Scale	Mean	Std. Dev.	LB	UB	Tolerance	p-value
Full	3.0065	0.013	2.9741	3.0389	0.0648	0.479
3/4	2.4415	0.1443	2.083	2.8	0.72	0.148
Half	1.5093	0.0103	1.4171	1.6014	0.1843	0.423

Failure Modes

Three distinct failure modes were identified for the plastic (Prusament PLA) risers: compression, layer collapse, and brittle crack; each fracture mode is pictured in Figure 15.

"Compression" was considered as a uniform progressive failure that occurs as the part yields under load. Compression failure modes were seen at the full-scale for 40% to 50%, at the three-quarter scale from 40% to 50%, and at the half-scale from 35% to 50% infill densities. "Layer collapse" indicated a cyclical failure that occurred as layers progressively collapsed under load. Layer collapse failure modes were seen at the full-scale from 30% to

Figure 15: Plastic failure modes: compression (left); layer collapse (middle); brittle crack (right).

35%, at the three-quarter scale for 15% and 25% to 35%, and at the half-scale from 10% to 30% infill densities. Finally, "brittle cracking" was a sudden catastrophic failure which occurred due to cracking along layer lines. Brittle cracking failure modes were seen at the full-scale from 5% to 25%, at the three-quarter scale from 5% to 10% and at 20%, and at the half-scale at 5% and 20% infill densities.

Generally speaking, compressive failure occurs at relatively higher infill densities, brittle cracking occurs at relatively lower infill densities, and layer collapse falls in the middle range of infill densities. Though some exceptions can be noted, e.g. layer collapse at 15% infill for three-quarter scale risers. The authors believe such discrepancies may be due to how the infill is distributed at the lower scales, and consequently where pockets of air at lower infill densities are positioned within the portion of the part receiving the load.

Regarding the wooden risers, four failure modes were identified: compression, paintbrushing, splitting, and mixed. The four failure modes are pictured in Figure 16.

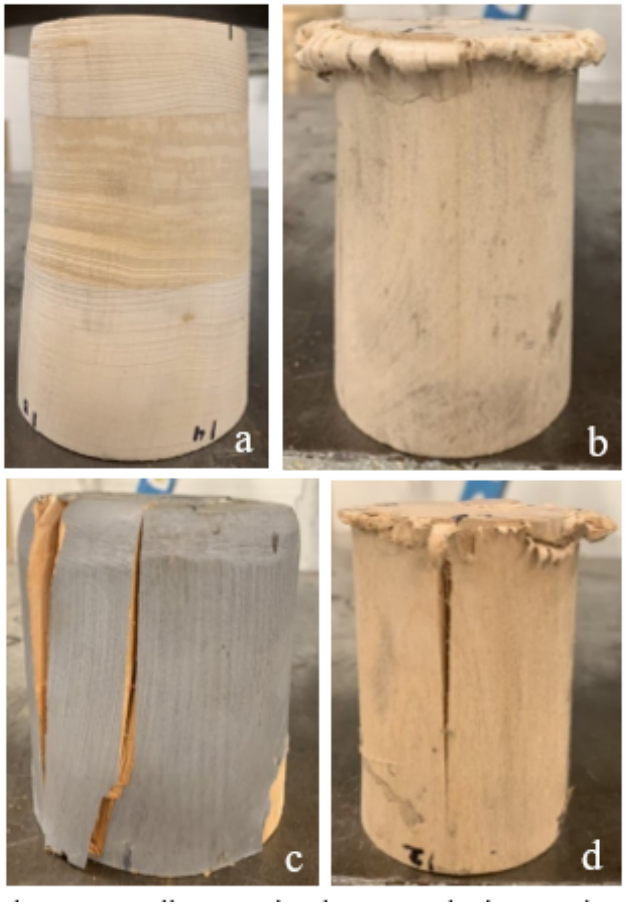

Figure 16: Failure mechanisms seen in the wooden risers (both coated and uncoated): (a) compression, (b) paintbrushing, (c) cracking, and (d) mixed.

Due to the smaller sample size, generalizations were more difficult to ascertain. However, compression failure modes seemingly related mostly to horizontal seams, whereas split and mixed failure modes mostly related to vertical seams.

Conclusions

Three initial DOEs and a full experimental study were conducted to answer the five research questions posed at the beginning of this case study. Regarding each of the research questions, the conclusions are as follows:

- RQ1: Does infill density (percentage) affect the print time, mass, compressive strength, dimensional stability, or surface roughness of additively manufactured risers of a standard length-to-diameter ratio?
  - Infill percentage significantly affected print time, height, diameter, mass, and compressive yield strength. Surface roughness was not found to be significantly affected by infill percentage, but the interaction between infill percentage and infill type significantly affected surface roughness.

- RQ2: Does shell thickness affect the print time, mass, compressive strength, dimensional stability, or surface roughness of additively manufactured risers of a standard length-to-diameter ratio?
  - Shell thickness did not significantly affect print time, mass, dimensional stability or surface roughness. It did significantly affect the compressive yield strength.
- RQ3: Does infill type (pattern) affect the print time, mass, compressive strength, dimensional stability, or surface roughness of additively manufactured risers of a standard length-to-diameter ratio?
  - Infill type significantly affected print time, height, diameter, mass, and compressive yield strength. It did not significantly affect surface roughness, but its interaction with infill percentage did.
- RQ4: Does filament color affect the print time, mass, compressive strength, dimensional stability, or surface roughness of additively manufactured risers of a standard length-to-diameter ratio?
  - Filament color did not significantly affect print time, mass, dimensional stability, or surface roughness of the risers. Filament color did significantly affect the compressive yield strength of the risers, favoring pineapple yellow.
- RQ5: What are the print time, mass, compressive strength, and dimensional stability capabilities at various infill densities of additively manufactured risers of a standard length-to-diameter ratio for a constant infill type, shell thickness, layer height, and filament color?
  - Holding the print type (cubic), shell thickness (0.7 mm), layer height (0.3 mm), and filament color (opal green) constant, the compressive yield strength generally increases with increasing infill percentage. Additionally, the compressive strength increases as the riser scale (full-scale, three-quarter scale, and half-scale) increases.

This case study served as a good first step to solving the issues associated with adopting additive manufacturing into the metalcasting patternmaking process. However, there were limitations to the study and therefore future work is necessary to paint a comprehensive portrait of the overall capabilities of AM in regards to applications for green sand metalcasting. The most logical next steps for this work are to extend the infill percentages past 50% and to consider different colors of Prusament PLA filaments using the same print settings. Additionally, investigation of the effects of other brands of filaments or printers would benefit the research since Prusament and Prusa i3 MK3S series printers are considered as rather high-end and unlikely to be as commonly purchased as less expensive brands of filaments and desktop printers. Comparison of other common infill patterns, such as gyroid, honeycomb, and grid, could be beneficial if their print times fall below and/or strengths significantly exceed that of standard cubic infill. Extended future work could include an exploration of additional material extrusion filaments such as polyethylene terephthalate glycol (PETG), acrylonitrile butadiene styrene (ABS), polypropylene (PP), and nylon. Carbon fiber-infused

and other composite-based filaments would also be interesting to investigate. Finally, research involving aging pattern parts would be beneficial to foundries, including the effects of sand abrasion on dimensional accuracy of AM risers, the effects of humidity and absorption of water on the dimensional accuracy and properties of AM risers, and the effects of using aging/opened filament rolls to print pattern parts.

Disclaimer

The data collected, analyses performed, and conclusions drawn are those of the authors and may not necessarily represent the opinions of Erie Bronze and Aluminum Company or any of its associated employees from the past, present, or future.

Acknowledgments

The authors would like to express their most sincere gratitude to several people at Erie Bronze and Aluminum Company for partnering with us on this project: Ms. Amber Evanoff for serving as the main contact throughout the project, Mr. Brad White for the tour of the facility, and Mr. Matthew Firster for answering all of our engineering questions and providing us with wooden pattern parts. Additionally, the following thank yous are due to faculty and staff of Penn State Behrend: Prof. Adam Wielobob for suggesting Erie Bronze as a local foundry for partnership, Mr. Chris Bartlett for machining off the runners from the old wooden risers, and the School of Engineering for access to the Tinius Olsen universal testing machine. Finally, the authors acknowledge Prof. Paul Lynch of the Materials and Manufacturing Research Group at Penn State Behrend for access to the group's Prusa 3D printers as well as providing the funding for the filament used in this case study.

References

[1] "AMO—Metal-Casting-August-2022-Public.pdf." Accessed: Jun. 26, 2023. [Online]. Available: https://science.osti.gov/-/media/sbir/pdf/Market-Research/AMO---Metal-Casting-August-2022-Public.pdf

[2] "Revisiting Metalcasting's Fascinating History Casting Source." https://www.castingsource.com/column/2019/08/16/revisiting-metalcastings-fascinating-history (accessed Jun. 26, 2023).

[3] "Reducing Sand Casting Lead Times and Production Costs With Hybrid 3D Printing — Casting Source." https://www.castingsource.com/articles/2023/01/31/reducing-sand-casting-lead-times-and-production-costs-hybrid-3d-printing (accessed Jun. 26, 2023).

[4] A. K. Elshennawy and G. S. Weheba, "Metal Casting Expendable Molds," Materials and Manufacturing Processes, 5th edn. Society of Manufacturing Engineers (SME), Southfield, pp. 159–198, 2015.

[5] H. W. Stoll, "Casting Design Issues and Practices," Dec. 2008, doi: 10.31399/asm.hb.v15.a0009014.

[6] B. V. Smith, "Introduction: Expendable Mold Processes with Expendable Patterns," Dec. 2008, doi: 10.31399/asm.hb.v15.a0005253.

[7] B. V. Smith, "Introduction: Expendable Mold Processes with Permanent Patterns," Dec. 2008, doi: 10.31399/asm.hb.v15.a0005241.

[8] Casting. 2008. doi: 10.31399/asm.hb.v15.9781627081870.

[9] G. Bardsley, "Traditional Casting Methods," Precision Investment Castings, Jun. 03, 2021. https://pi-castings.co.uk/traditional-casting-methods/ (accessed Jun. 26, 2023).

[10] T. Sivarupan et al., "A review on the progress and challenges of binder jet 3D printing of sand moulds for advanced casting," Additive Manufacturing, vol. 40, p. 101889, Apr. 2021, doi: 10.1016/j.addma.2021.101889.

[11] "ExOne's Family of Sand 3D Printers." https://www.exone.com/en-US/3D-printing-systems/sand-3d-printers (accessed Jun. 26, 2023).

[12] "3D Sand Printing for Casting Molds & Cores," Voxeljet. https://www.voxeljet.com/3d-printing-solution/sand-casting/ (accessed Jun. 26, 2023).

[13] P. Lynch, C. Hasbrouck, J. Wilck, M. Kay, and G. Manogharan, "Challenges and opportunities to integrate the oldest and newest manufacturing processes: metal casting and additive manufacturing," Rapid Prototyping Journal, vol. 26, no. 6, pp. 1145–1154, Jun. 2020, doi: 10.1108/RPJ-10-2019-0277.

[14] C. A. Lawton, "What is the process for designing a pattern?," The C.A. Lawton Co., Jan. 22, 2020. https://calawton.com/pattern-design-process/ (accessed Jun. 26, 2023).

[15] "Introduction to Metal Casting and Ways to Combine 3D Printing With Casting Workflows," Formlabs. https://formlabs.com/blog/metal-casting/ (accessed Jun. 26, 2023).

[16] "Using a Complexity Factor to Calculate Cost Benefits of 3-D Sand Printing — Modern Casting." https://www.moderncasting.com/articles/2017/04/20/using-complexity-factor-calculate-cost-benefits-3-d-sand-printing (accessed Jun. 26, 2023).

[17] M. Firster, "Interview with Firster," 2022.

[18] C. Scott, "material extrusion 3D Printing as an Alternative Form of Making Patterns for Sand Casting Learnings from the Shop Floor," 3DPrint.com — The Voice of 3D Printing / Additive Manufacturing, Aug. 20, 2018. https://3dprint.com/222949/3d-printing-patterns-sand-casting/ (accessed Jun. 26, 2023).

[19] C. R. Hasbrouck, J. W. Fisher, M. R. Villalpando, and P. C. Lynch, 'A Comparative Study of Dimensional Tolerancing Capabilities and Microstructure Formation between Binder Jet Additively Manufactured Sand Molds and Olivine Green Sand Molds for Metalcasting of A356.0,' Procedia Manuf., vol. 48, pp. 338–348, 2020.

[20] P. Anakhu, C. Bolu, A. Abioye, and J. Azeta, "Fused Deposition Modeling Printed Patterns for Sand Casting in a Nigerian Foundry: A Review," International Journal of Applied Engineering Research, vol. 13, Jan. 2018.

[21] "Compressive Strength Assessment of 3D Printing Infill Patterns - ScienceDirect." https://www.sciencedirect.com/science/article/pii/S2212827122001159 (accessed Jun. 26, 2023).

[22] D. Harshit et al., "Compressive Strength of PLA Based Scaffolds: Effect of Layer Height, Infill Density and Print Speed" Accessed: Jun. 26, 2023. [Online]. Available: https://ijmmt.ro/vol11no12019/03HarshitDave.pdf

[23] K. Chin Ang, K. Fai Leong, C. Kai Chua, and M. Chandrasekaran, "Investigation of the mechanical properties and porosity relationships in fused deposition modelling-fabricated porous structures," Rapid Prototyping Journal, vol. 12, no. 2, pp. 100–105, Jan. 2006, doi: 10.1108/13552540610652447.

[24] H. Chim et al., "A comparative analysis of scaffold material modifications for load-bearing applications in bone tissue engineering," International Journal of Oral and Maxillofacial Surgery, vol. 35, no. 10, pp. 928–934, Oct. 2006, doi: 10.1016/j.ijom.2006.03.024.

[25] 'Investigation of Sparse-Build Rapid Tooling by Fused Deposition Modeli' by Osman Iyibilgin, Ming-Chuan Leu et al. https://scholarsmine.mst.edu/mecaerengfacwork/4750/(accessed Jun. 26, 2023).

[26] A. K. Sood, R. K. Ohdar, and S. S. Mahapatra, "Experimental investigation and empirical modelling of material extrusion process for compressive strength improvement," Journal of Advanced Research, vol. 3, no. 1, pp. 81–90, Jan. 2012, doi: 10.1016/j.jare.2011.05.001.

[27] "Determination and Comparison of the Anisotropic Strengths of Fused Deposition Modeling P400 ABS SpringerLink." https://link.springer.com/chapter/10.1007/978-981-10-0812-22 (accessed Jun. 26, 2023).

[28] S. Ahn, M. Montero, D. Odell, S. Roundy, and P. K. Wright, "Anisotropic material

properties of fused deposition modeling ABS," Rapid Prototyping Journal, vol. 8, no. 4, pp. 248–257, Jan. 2002, doi: 10.1108/13552540210441166.

[29] H. Jami, S. H. Masood, and W. Q. Song, "Dynamic stress-strain compressive behaviour of material extrusion made ABS and PC parts under high strain rates," IOP Conf. Ser.: Mater. Sci. Eng., vol. 377, no. 1, p. 012153, Jun. 2018, doi: 10.1088/1757-899X/377/1/012153.

[30] "A numerical and experimental study of the compression uniaxial properties of PLA manufactured with material extrusion technology based on product specifications SpringerLink." https://link.springer.com/article/10.1007/s00170-019-03626-0 (accessed Jun. 26, 2023).

[31] "The fracture mechanism of polylactic acid resin and the improving mechanism of its toughness by addition of acrylic modifier - Ito - 2010 - Journal of Applied Polymer Science - Wiley Online Library." https://onlinelibrary.wiley.com/doi/abs/10.1002/app.31292 (accessed Jun. 26, 2023).

[32] A. Lanzotti, M. Grasso, G. Staiano, and M. Martorelli, "The impact of process parameters on mechanical properties of parts fabricated in PLA with an open-source 3-D printer," Rapid Prototyping Journal, vol. 21, no. 5, pp. 604–617, Jan. 2015, doi: 10.1108/RPJ-09-2014-0135.

[33] "Impact of Infill Design on Mechanical Strength and Production Cost in Material Extrusion Based Additive Manufacturing - ProQuest. https://www.proquest.com/openview/1b0d2751a98143f75b835a1df22bf70b/1?pq-origsite=gscholar&cbl=18750&diss=y (accessed Jun. 26, 2023).

[34] "Manufacturing PA Initiative," PA Department of Community and Economic Development. https://dced.pa.gov/business-assistance/technology-innovation/manufacturing-pa-initiative/ (accessed Jun. 26, 2023).

[35] B. White, "Interview with White," 2022.

[36] R. C. Voigt, "Patterns and Patternmaking," Dec. 2008, doi: 10.31399/asm.hb.v15.a0005308.

[37] Basic Principles of Gating and Risering, 2nd ed. American Foundry Society, 2008.

[38] N. Chvorinov, "Theory of solidifcation of castings," Giesserei, vol. 27, pp. 177–225, 1940.

[39] "Fused Filament Fabrication of Ceramic Components for Home Use SpringerLink." https://link.springer.com/chapter/10.1007/978-3-030-62784-311 (accessed Jun. 26, 2023).

[40] "PLA Glitter - Spectrum Filaments," Sep. 19, 2021. https://spectrumfilaments.com/en/filament/pla-glitter/ (accessed Jun. 26, 2023).

[41] K. Stevenson, "Really, How Bad Are Abrasive Filaments For Your 3D Printer Nozzle? ≪Fabbaloo," Fabbaloo, Oct. 26, 2019. https://www.fabbaloo.com/2019/10/really-how-bad-are-abrasive-filaments-for-your-3d-printer-nozzle (accessed Jun. 26, 2023).

[42] D. W. Green, J. E. Winandy, and D. E. Kretschmann, "Mechanical properties of wood," Wood handbook: wood as an engineering material. Madison, WI: USDA Forest Service, Forest Products Laboratory, 1999. General technical report FPL; GTR-113: Pages 4.1-4.45, vol. 113, 1999, Accessed: Jun. 26, 2023. [Online]. Available: https://www.fs.usda.gov/research/treesearch/7149

[43] S. Dev and R. Srivastava, "Effect of infill parameters on material sustainability and mechanical properties in fused deposition modelling process: a case study," Prog Addit Manuf, vol. 6, no. 4, pp. 631–642, Dec. 2021, doi: 10.1007/s40964-021-00184-4.

[44] A. Pandžić, D. Hodzic, and A. Milovanović, "Influence of Material Colour on Mechanical Properties of PLA Material in material extrusion Technology," Oct. 2019, doi: 10.2507/30th.daaam.proceedings.075.